THE ASTROPHYSICAL JOURNAL, 277:92–105, 1984 February 1

NEUTRAL HYDROGEN IN SEYFERT GALAXIES

I. F. MIRABEL
Department of Physics, University of Puerto Rico
AND
A. S. WILSON
Astronomy Program, University of Maryland
Received 1982 December 7; accepted 1983 June 13

ABSTRACT

We report a single-dish survey for neutral hydrogen in 91 Seyfert or Seyfert-like galaxies, most of which have redshifts below 12,000 km s^{-1}. H I emission has been detected in 39 galaxies and H I absorption in two. The redshifts obtained from the nuclear optical emission lines are systematically smaller than the systemic velocities derived from the H I emission-line profiles. The mean difference is about 60 km s^{-1}. This effect is probably not a consequence of systematic errors in the velocities but arises from a net outflow of gas in the narrow emission-line regions. For the majority of Seyfert galaxies, the ratio of hydrogen mass to blue luminosity (M_H/L_B) does not differ from the values expected for a normal galaxy of the same morphological type. There are, however, seven cases of very gas-rich Seyfert galaxies with $M_H/L_B > 0.4$. Several instances are known in which the H I absorption line is redshifted with respect to the systemic velocity, suggesting that infall of H I and/or strong noncircular motions are common processes. A considerable fraction, perhaps 40% or more, of Seyfert galaxies exhibits H I profiles different from the typical profiles of normally rotating spiral galaxies. This result is ascribed either to blended emission from more than one galaxy in the beam or to perturbations of the internal dynamics of the galaxies by tidal interactions with close companions.

Subject headings: galaxies: Seyfert — galaxies: structure — radio sources: galaxies — radio sources: 21 cm radiation

I. INTRODUCTION

The properties of the disks of active galaxies are of interest in identifying the origin of their energetic nuclear phenomena. Studies of the galaxy morphologies show the general occurrence of radio emission in elliptical galaxies and of the Seyfert phenomenon in early-type spirals, indicating the importance of a bulge component for nuclear activity. Simkin, Su, and Schwarz (1980) have suggested that Seyfert galaxies are characterized by other morphological peculiarities, such as inner and outer rings and a three-step optical brightness structure—an inner disk or ring, an intermediate envelope, bar, or lens, and a faint outer envelope, ring, or pseudo-ring.

It is often proposed that nuclear activity is powered by accretion of gas from the nuclear environment. Thus studies of the gaseous component of the galaxy hold out the possibility of identifying the cause of the noncircular motions (e.g., bars, tidal disruption by companion galaxies, etc.) which allow gas to fall into the nucleus. Optical mapping of the dynamics of the gaseous components of the disks of Seyfert galaxies requires considerable amounts of large-telescope time even if emission lines are detectable throughout the disk. Radio detection of CO emission is feasible only for a few nearby Seyfert galaxies, but a promising approach involves 21 cm H I line observations. The first single-dish H I survey of a significant number of Seyfert galaxies was performed by Heckman, Balick, and Sullivan (1978, hereafter HBS). They surveyed 58 galaxies and detected, or probably detected, H I emission in 25, of which 19 are currently classified as Seyfert galaxies. Since this survey, the number of known Seyfert galaxies has grown to well over 200, and, with the continued improvement in the quality of 21 cm line receivers, it seemed worthwhile to perform a new survey of this type of object.

In the present paper, we report a single-dish H I survey of 91 Seyfert and Seyfert-like galaxies, selected from the lists of Weedman (1977, 1978) and Huchra (1982). H I emission has been detected in 39 galaxies and H I absorption in two. The observed galaxies are located north of $\delta = -19°$, and all but nine have recession velocities below 12,000 km s^{-1}. The aims of our survey were to expand the data base on the H I properties of Seyferts, to compare their properties with non-Seyfert galaxies, to search for clues as to the origin of activity, and to correlate H I with nuclear properties in the other wave bands. We were also interested in the identification of galaxies with strong or unusual H I signals for subsequent mapping with aperture-synthesis instruments.

Section II describes our observing technique, and in § III we present the results. Section IV is devoted to a discussion of the results and their implications. Throughout the paper, distance-related quantities have been computed using a Hubble constant $H_0 = 55$ km s^{-1} Mpc^{-1}.

II. OBSERVATIONS

The H I observations were made using the 305 m radio telescope of the Arecibo Observatory[1] during 1980 April and

[1] The Arecibo Observatory is part of the National Astronomy and Ionosphere Center (NAIC), which is operated by Cornell University under contract with the National Science Foundation.

1981 September, and the 91 m radio telescope of the National Radio Astronomy Observatory[2] during 1981 November.

At Arecibo, a 12 m line feed, sensitive to left- and right-circular polarization, was used. The resolution was 3.'3 (FWHM), and typical system temperatures of 100 and 40 K for the 1980 April and 1981 September observations, respectively, were obtained. Spectra were taken with a 1008 channel autocorrelation spectrometer, split into two banks of 504 channels each. The total bandwidth was 10 MHz ($\sim$2100 km s^{-1}), and the channel spacing was 19.5 kHz ($\sim$4.2 km s^{-1}), although the spectra presented here have been smoothed over three channels. The system was calibrated each day by means of continuum radio sources of known flux density at 1400 MHz, and galaxies with well-studied H I profiles were observed regularly in order to check the calibration procedure. The system response deteriorates toward large zenith distances, so corrections for zenith angle and frequency dependence were applied. We estimate that calibration uncertainties for the 305 m observations introduce a maximum error of $\pm 25\%$ in the H I fluxes.

At the 91 m telescope, orthogonal linear polarizations were fed into dual, cooled field effect transistor receivers, each having a system temperature of 50 K. The resolution was 10.'8 (FWHM), and a 384 channel autocorrelation spectrometer, split into two banks of 192 channels each, was used. The total bandwidth was 10 MHz, and the channel spacing was 11 km s^{-1}. These NRAO spectra have been Hanning smoothed once, yielding a resolution of $\sim$22 km s^{-1}. The system calibration was achieved with continuum radio sources of well-known flux density, and the uncertainty in the H I fluxes due to calibration errors is estimated at $\pm 20\%$.

Spectra affected by the Sun or strong continuum sources provide very uncertain results and are not considered in the present study. All observations were reduced using standard spectral-line software available at Arecibo and NRAO.

III. RESULTS

The Arecibo spectra of 26 detected or marginally detected galaxies are given in Figure 1*a*, with the corresponding NRAO results for 15 galaxies in Figure 1*b*. As noted in § II, the Arecibo data have been smoothed with a boxcar function of width 3 channels, and the NRAO data have been Hanning smoothed once. The spectra of NGC 3227, NGC 7469, and NGC 7714 were obtained as part of a survey of H I in bright galaxies with strong radio sources (Mirabel 1982). The galaxy Mrk 348 was observed with both telescopes, and each spectrum is shown. The integrated hydrogen flux density of this galaxy measured at NRAO is 2.5 times that measured at Arecibo; this result is consistent with the large angular extent of the H I in Mrk 348 (Morris and Wannier 1980; Heckman *et al.* 1982). The galaxies NGC 931, NGC 3227, and NGC 4235 have optical sizes larger than the 3.'3 Arecibo telescope beam, so the measured H I flux densities must be considered lower limits.

Table 1, which contains the observational results and notes on individual galaxies, is arranged as follows:

Col. (1).—Galaxy running number followed, in parentheses, by the diameter in meters of the telescope used for the H I observations. The galaxy names that correspond to the running numbers in Table 1 are given in the key to the table. Alternate designations for each galaxy are given in the notes. Asterisks indicate galaxies that probably are not Seyfert.

Col. (2).—Right ascension and declination in 1950.0 coordinates. The positions were taken from Clements (1981, 1982), Wilson and Meurs (1978), Kojoian, Elliott, and Tovmassian (1978), Tovmassian, Shahbazian, and Kandalian (1980), Joshi and Kandalian (1981), Peterson (1973), Dressel and Condon (1976), Gallouët, Heidmann, and Dampierre (1975), and Apparao *et al.* (1978). The accuracy of these measurements ranges from $\pm 0.''2$ (Clements 1981, 1982) to a few arc seconds, although the positions quoted in Table 1 have been rounded to the nearest tenth of a second in right ascension and to the nearest arc second in declination.

Col. (3).—Photographic magnitude, m_p, as given by Zwicky *et al.* (1961–1968), Zwicky (1971), the original Markarian surveys, or Huchra (1982).

Col. (4).—Face-on angular diameter, $a_H(0)$, in arc minutes, on the Holmberg scale. Measurements of the major axis a and axial ratio $r = b/a$ were first obtained (see below). The major axis was converted to the Holmberg system (a_H) by means of the equation

$$\log a_H = 0.81 \log a + 0.26 ; \quad (1)$$

a_H was then corrected to the face-on diameter $a_H(0)$ through

$$\log a_H(0) = \log a_H - 0.3 \log (1/r_H) , \quad (2)$$

where $r_H = b_H/a_H$ is the axial ratio in the Holmberg system (cf. Sullivan *et al.* 1981). The ratio r_H was calculated from the measured ratio r with (Fisher and Tully 1981)

$$r_H = 0.91r + 0.09 . \quad (3)$$

Col. (5).—Inclination, i, between the plane of the galaxy and the sky, measured in degrees, and computed from

$$\cos^2 i = (r_H^2 - r_0^2)/(1 - r_0^2) , \quad (4)$$

where r_0 (=0.2) is the intrinsic axial ratio of the light distribution (e.g., Sullivan *et al.* 1981).

Equations (1) and (3) are, strictly speaking, applicable only to diameters a and ratios r obtained from the *Uppsala General Catalogue of Galaxies* (UGC, Nilson 1973), and this catalog was our primary source (cf. Sullivan *et al.* 1981; Fisher and Tully 1981). For galaxies not listed in the UGC, diameters were taken from the RCBG2 (de Vaucouleurs, de Vaucouleurs, and Corwin 1976) or the original Markarian lists. Axial ratios were also culled from Keel (1980), Simkin, Su, and Schwarz (1980), and Su and Simkin (1980). When no measurements were available in the literature, a and r were determined directly from the Palomar Sky Survey (PSS) prints. In view of the uncertainties in the correction from measurements in other systems to the Holmberg system, equations (1)–(4) have been used in all cases. Values of $a_H(0)$ and i are followed by the symbol $^+$ when they have not been derived from the UGC. Such is mainly the case for galaxies smaller than 1′ in size. Some galaxies are very compact or are highly distorted, and no values are given in columns (4) or (5) for these systems. Among galaxies

[2] The NRAO is operated by Associated Universities, Inc., under contract with the National Science Foundation.

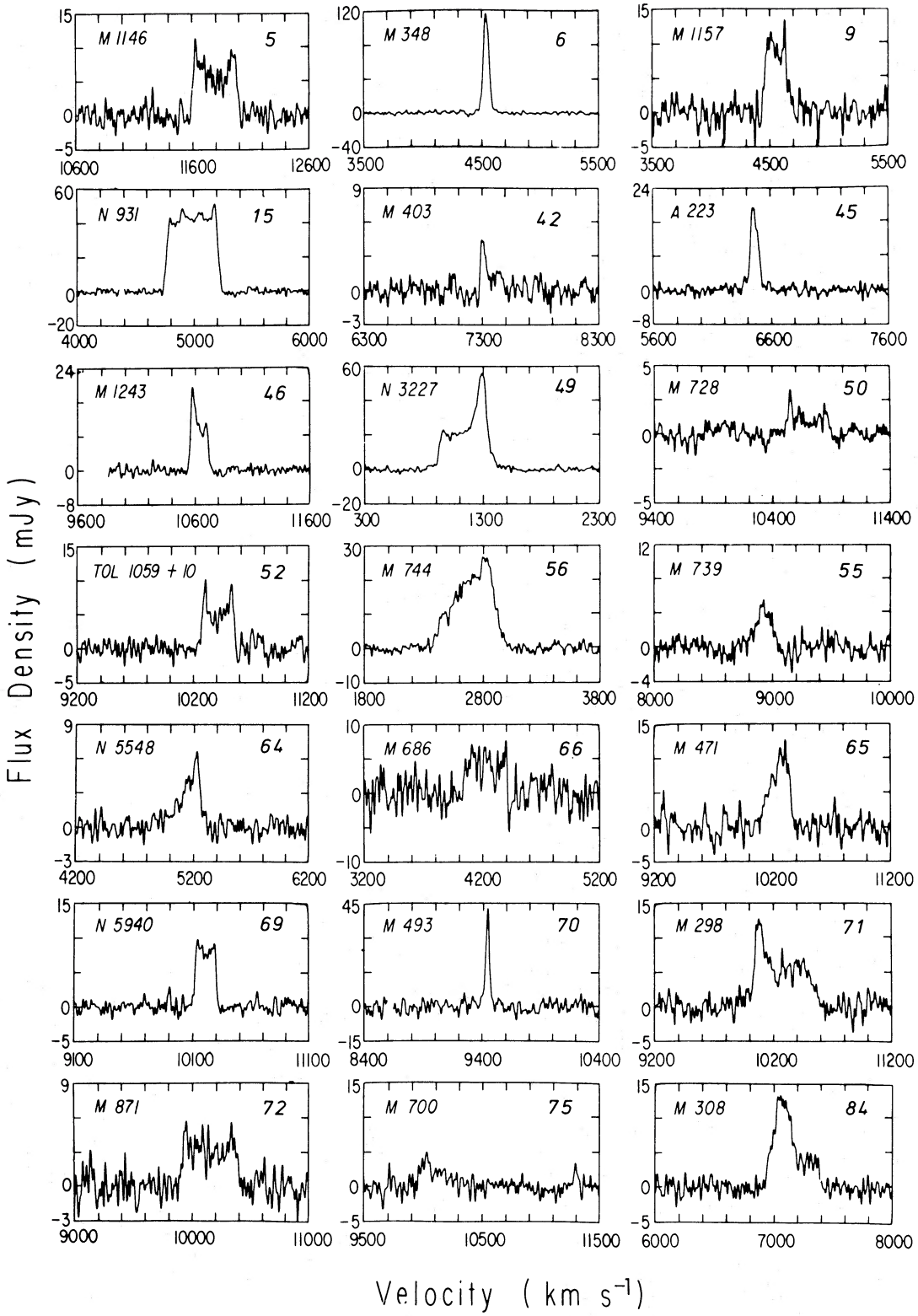

FIG. 1*a*.—H I profiles of detected and marginally detected galaxies obtained with the 305 m radio telescope of the Arecibo Observatory. Ordinate is flux density (mJy) and abscissa is heliocentric redshift (km s^{-1}). Tick marks in the abscissa are spaced every 200 km s^{-1}. The galaxy name is given at the top on the left side. The running number of Table 1 is given on the right side.

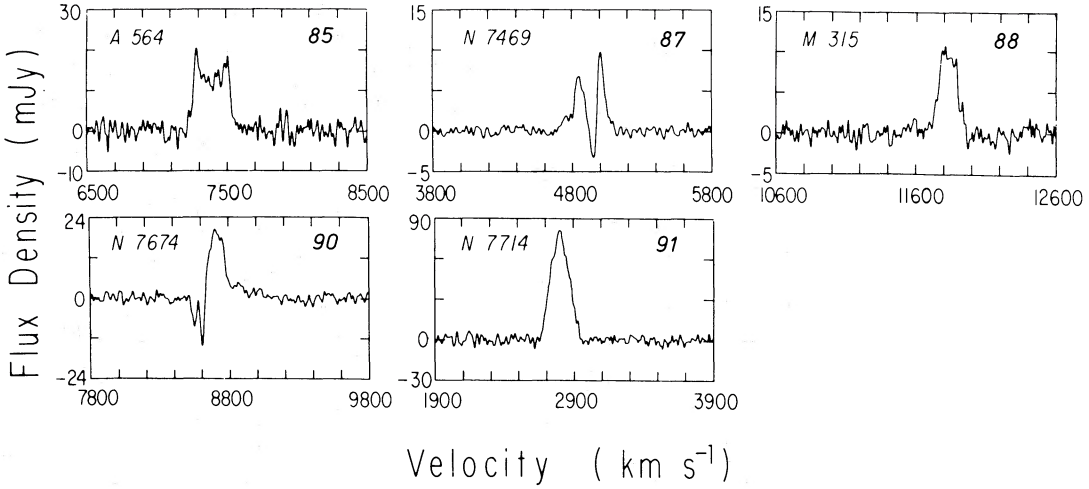

FIG. 1*a*—*Continued*

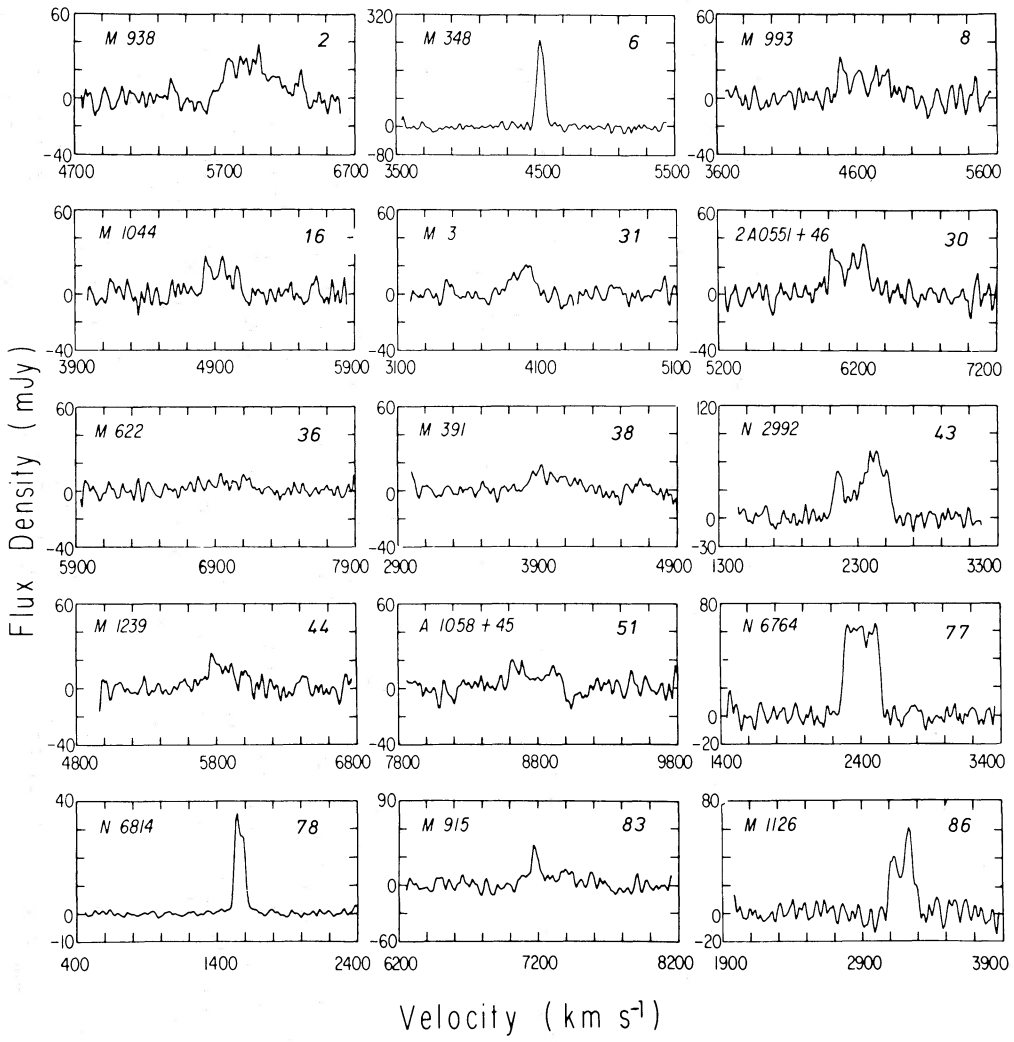

FIG. 1*b*.—H I profiles of detected and marginally detected galaxies obtained with the 91 m radio telescope of the NRAO. The ordinate and abscissa are the same as in Fig. 1*a*.

TABLE 1

PROPERTIES OF OBSERVED SEYFERT GALAXIES

	Galaxy (1)	R.A. (1950) (2)	Decl. (1950)	m_p (3)	$a_H(0)$ (′) (4)	i (°) (5)	V_{opt} (km s^{-1}) (6)	V_{HI} (km s^{-1}) (7)
1	(305)	00^{h}03^{m}45^s.2	19°55′29″	14.0	...	...	7757	...
2	(91)	00 08 33.7	−12 23 13	14.0	...	...	5753	5931
3	(91)	00 23 21.3	−03 41 50	15.0	0.60$^+$	35$^+$	4398	...
4	(91)	00 35 02.0	00 00 27	15.4	...	...	10,424	...
5	(305)	00 44 42.2	14 25 50	15.2	1.64	47	11,667	11,787
6	(305)	00 46 04.9	31 41 05	15.0	2.64	14	4546	4538
6	(91)	00 46 04.9	31 41 05	15.0	2.64	14	4546	4540
7	(305)	01 21 56.3	31 54 20	14.2	1.89	30	10,800	...
8	(91)	01 22 42.5	31 52 33	14.0	2.90	72	4625	4662
9	(305)	01 30 38.8	35 24 43	14.0	2.24	37	4558	4554
10	(91)	01 37 35.7	31 59 38	15.8	...	...	19,620	...
11	(305)	01 41 22.9	02 05 56	14.0	2.75	19	5178	...
12	(91)	02 03 42.5	−00 31 47	14.6	2.01	32	12,693	...
13	(91)	02 12 00.4	−00 59 57	14.0	2.25	0	7891	...
14	(91)	02 14 19.8	38 10 59	13.6	1.20	75	5285	...
15	(305)	02 25 16.5	31 05 18	13.9	4.45	74	4910	4990
16	(91)	02 27 38.7	−09 13 13	14.5	0.61$^+$	49$^+$	4900	4932
17	(305)	02 35 52.3	01 41 32	14.6	1.90	26	7251	...
18	(91)	02 41 00.7	62 15 27	17.8	...	...	13,200	...
19	(305)	02 38 55.8	06 58 27	15.0	0.52$^+$	51$^+$	7792	...
20	(305)	02 46 46.9	34 46 53	15.4	...	...	5190	...
21	(305)	02 56 49.8	36 37 21	13.8	2.99	37	3610	...
22	(91)	03 11 42.8	41 51 03	14.0	1.75	30	7041	...
23	(91)	03 22 57.3	−06 19 09	14.5	...	52	9000	...
24	(91)	03 28 09.9	−03 18 35	15.5	0.44$^+$	60$^+$	6002	...
25	(91)	03 35 57.3	09 48 27	16.5	...	...	10,458	...
26	(91)	04 33 59.9	−10 28 36	14.5	0.38$^+$	50$^+$	10,406	...
27	(91)	05 07 08.0	07 25 16	15.6	1.55	78	5689	...
28	(91)	05 13 37.9	−00 12 15	14.6	2.20	42	9798	...
29	(91)	05 49 46.4	−07 28 02	14.0	...	...	2307	...
30	(91)	05 51 09.7	46 25 51	13.9	4.06	26	6012	6146
31	(91)	06 09 48.4	71 03 11	13.8	2.79	26	4091	3957
32	(91)	06 45 43.9	74 29 10	14.8	1.60	51	5536	...
33	(91)	06 55 34.6	54 15 57	15.5	0.27$^+$	61$^+$	13,043	...
34	(91)	07 32 42.1	58 52 56	15.2	0.89$^+$	19$^+$	11,895	...
35	(91)	07 37 56.8	65 17 42	15.0	0.58$^+$	63$^+$	11,136	...
36	(91)	08 04 21.2	39 09 01	14.4	1.20	0	7000	6964
37	(305)	08 35 13.1	25 04 16	14.8	1.02$^+$	57$^+$	8564	...
38	(91)	08 51 32.3	39 43 46	13.9	2.42	44	3896	3991
39	(305)	09 15 39.4	16 30 59	15.2	0.58$^+$	66$^+$	8796	...
40	(91)	09 21 44.3	52 30 07	16.0	0.39$^+$	72$^+$	10,465	...
41	(305)	09 23 20.0	12 57 04	13.9	1.15	31	8637	...
42	(305)	09 37 55.7	21 27 43	15.4	...	...	7206	7356
43	(91)	09 43 17.6	−14 05 45	13.0	1.53$^+$	67$^+$	2305	2350
44	(91)	09 49 46.3	−01 22 36	14.5	...	...	6108	5834
45*	(305)	09 54 42.8	07 25 39	15.0	0.49$^+$	...	6600	6459
46	(305)	09 57 14.2	13 17 05	14.5	1.80	18	10,602	10,629
47	(305)	10 04 55.3	17 20 43	15.1	...	...	7800	...
48	(91)	10 15 39.3	64 13 06	15.2	0.52$^+$	37$^+$	11,700	...
49	(305)	10 20 46.8	20 07 06	12.2	6.72$^+$	47$^+$	1152	1146
50	(305)	10 58 24.9	11 19 00	16.0	0.47$^+$	...	10,722	10,686
51	(91)	10 58 42.5	45 55 22	14.1	1.50	47	8778	8718
52	(305)	10 59 21.0	10 33 48	15.5	...	...	10,248	10,414
53	(91)	11 03 22.8	72 50 20	12.3	3.12	30	2540	...
54	(305)	11 24 07.6	35 31 34	14.9	0.77$^+$	49$^+$	9789	...
55	(305)	11 33 52.8	21 52 22	14.8	...	...	8890	8912
56	(305)	11 37 04.9	32 11 11	13.5	2.94	59	2737	2707
57	(91)	11 58 40.6	−03 23 59	16.5	...	...	5694	...
58	(305)	12 01 56.3	20 35 40	15.4	...	59	6600	...
59	(305)	12 14 36.7	07 28 09	13.2	3.70	79	2300	...
60	(305)	12 15 55.6	30 05 26	13.7	1.60	41	3836	...
61	(305)	12 20 50.7	02 57 22	15.5	...	...	7013	...
62	(305)	13 29 55.4	11 21 44	14.5	...	...	9318	...
63	(305)	13 38 54.0	30 37 49	15.3	0.43$^+$	52$^+$	12,287	...
64	(305)	14 15 43.5	25 22 01	13.1	2.67	31	4981	5142

TABLE 1—*Continued*

F_H ($10^6 M_\odot$ Mpc^{-2}) (8)	ΔV_{20} (km s^{-1}) (9)	$\Delta V_{20}(0)$ (km s^{-1}) (10)	M_H ($10^9 M_\odot$) (11)	L_B ($10^{10} L_\odot$) (12)	M_i ($10^{10} M_\odot$) (13)	M_H/L_B (14)	M_H/M_i (in solar units) (15)	M_i/L_B (16)
<0.13	...	...	<2.7	10.2	...	<0.03	...	...
2.4 ± 0.8	514	...	28.3	5.2	...	0.54	...	...
<0.38	...	...	<2.6	1.6	...	<0.16	...	...
<0.31	...	...	<11.4	6.1	...	<0.19	...	...
0.61 ± 0.12	418	571	30.3	10.6	58.1	0.29	0.05	5.5
1.65 ± 0.09	110	...	16.0	3.3	...	...	...	...
4.11 ± 0.31	120	...	30.7	3.3	...	0.93	...	...
<0.21	...	...	<9.2	19.9	...	<0.05	...	...
1.44 ± 0.57	391	411	11.4	7.4	21.5	0.15	0.05	2.9
0.45 ± 0.12	318	528	3.7	4.6	26.9	0.08	0.01	5.8
<0.42	...	...	<54.5	18.7	...	<0.29	...	...
<0.17	...	...	<2.0	6.0	...	<0.03	...	...
<0.38	...	...	<20.4	16.9	...	<0.12	...	...
<0.99	...	...	<21.1	9.9	...	<0.21	...	...
<0.50	...	...	<4.9	16.8	...	<0.03	...	...
4.65 ± 0.17	489	509	52.7	13.0	53.0	0.41	0.10	4.1
0.99 ± 0.33	258	342	8.1	2.9	3.2	0.28	0.25	1.1
<0.28	...	...	<5.6	5.4	...	<0.10	...	...
<0.52	...	...	<30.9	50.3	...	0.06	...	...
<0.14	...	...	<2.8	5.5	...	<0.05	...	...
<0.14	...	...	<1.3	2.1	...	<0.06	...	...
<0.17	...	...	<1.0	4.9	...	<0.02	...	...
<0.35	...	...	<6.0	15.6	...	<0.04	...	...
<0.83	...	...	<22.0	10.4	...	<0.21	...	...
<0.45	...	...	<5.3	2.4	...	<0.22	...	...
<0.33	...	...	<11.9	2.9	...	<0.41	...	...
<0.47	...	...	<17.9	14.3	...	<0.13	...	...
<0.40	...	...	<4.2	4.6	...	<0.09	...	...
<0.35	...	...	<11.2	13.8	...	<0.08	...	...
<0.45	...	...	<0.7	1.1	...	<0.06	...	...
1.86 ± 0.64	429	...	24.9	21.4	...	0.12	...	...
0.85 ± 0.35	250	...	4.9	6.0	...	0.08	...	...
<0.26	...	...	<2.7	4.0	...	<0.07	...	...
<0.33	...	...	<19.2	14.7	...	<0.13	...	...
<0.26	...	...	<12.0	11.3	...	<0.11	...	...
<0.38	...	...	<16.0	14.9	...	<0.11	...	...
0.64 ± 0.40	380	...	10.2	6.7	...	0.15	...	...
<0.12	...	...	<3.0	8.6	...	<0.03	...	...
0.92 ± 0.38	362	521	4.9	3.0	23.2	0.16	0.02	7.7
<0.10	...	...	<2.4	7.4	...	<0.03	...	...
<0.54	...	...	<21.0	7.0	...	<0.30	...	...
<0.08	...	...	<1.8	13.4	...	<0.01	...	...
0.09 ± 0.02	212	...	1.6	2.9	...	0.06	...	...
4.30 ± 0.71	428	465	6.3	2.4	6.2	0.26	0.10	2.6
1.11 ± 0.45	360	...	12.9	4.1	...	0.31	...	...
0.38 ± 0.05	236	...	4.9	3.3	...	0.15	...	...
0.45 ± 0.05	189	...	18.5	12.3	...	0.15	...	...
<0.07	...	...	<1.4	4.1	...	<0.03	...	...
<0.24	...	...	<11.1	9.9	...	<0.11	...	...
3.02 ± 0.17	526	722	3.1	1.4	33.4	0.22	0.01	...
0.12 ± 0.05	393	...	4.5	3.9	...	0.12	...	...
0.94 ± 0.52	375	513	24.0	12.6	31.6	0.19	0.08	2.5
0.38 ± 0.07	295	...	13.3	5.2	...	0.26	...	...
<0.66	...	...	<1.6	6.1	...	<0.03	...	...
<0.14	...	...	<4.3	8.5	...	<0.05	...	...
0.17 ± 0.07	340	...	4.4	6.5	...	0.07	...	...
2.15 ± 0.17	644	751	6.5	2.1	41.0	0.31	0.02	19.5
<0.47	...	...	<4.8	0.7	...	<0.69	...	...
<0.19	...	...	<2.7	2.9	...	<0.09	...	...
<0.26	...	...	<0.5	3.2	...	<0.02	...	...
<0.12	...	...	<0.6	3.0	...	<0.02	...	...
<0.17	...	...	<2.7	2.4	...	<0.11	...	...
<0.07	...	...	<2.0	9.0	...	<0.02	...	...
<0.09	...	...	<4.5	10.2	...	<0.04	...	...
0.24 ± 0.07	472	...	2.7	9.0	...	0.03	...	...

TABLE 1—*Continued*

Galaxy (1)	R.A. (1950) (2)	Decl. (1950)	m_p (3)	$a_H(0)$ (′) (4)	i (°) (5)	V_{opt} (km s^{-1}) (6)	V_{HI} (km s^{-1}) (7)
65 (305)	14 20 46.9	33 04 37	14.5	1.48	49	10,200	10,254
66 (305)	14 35 19.7	36 47 02	13.9	2.43	43	4209	4225
67 (305)	15 01 36.3	10 37 56	14.0	...	...	10,921	...
68 (305)	15 27 37.9	30 39 23	15.1	...	...	10,453	...
69 (305)	15 28 51.3	07 37 38	14.3	1.52	0	10,160	10,205
70 (305)	15 57 16.3	35 10 15	14.9	2.25	0	9386	9442
71 (305)	16 03 21.9	17 56 11	15.2	2.20	...	10,245	10,241
72 (305)	16 06 13.9	12 28 00	14.9	0.55^+	72^+	10,100	10,144
73 (305)	16 27 47.1	24 33 07	15.5	...	...	11,389	...
74 (305)	16 59 10.4	29 28 43	17.0	...	43	11,000	...
75 (305)	17 01 21.6	31 31 39	15.4	...	...	10,500	...
76 (305)	17 20 45.5	30 55 39	15.3	0.78^+	46^+	12,932	...
77 (91)	19 07 01.2	50 51 08	13.2	3.11	52	2405	2407
78 (91)	19 39 55.8	−10 26 33	11.9	1.89^+	21^+	1437	1561
79 (91)	20 41 26.2	−10 54 18	13.0	...	...	10,358	...
80 (91)	20 43 44.5	−02 59 46	16.0	0.62^+	...	8000	...
81 (91)	21 30 01.1	09 55 01	14.3	0.78	65	18,315	...
82 (91)	22 14 45.9	13 59 20	14.6	...	...	19,707	...
83 (91)	22 34 07.3	−12 48 18	15.0	0.82^+	55^+	7225	7248
84 (305)	22 39 30.5	19 59 59	14.7	0.62^+	46^+	6998	7121
85 (305)	22 40 18.3	29 27 48	14.4	1.33	52	7200	7390
86 (91)	22 58 10.0	−13 11 14	14.5	0.87^+	43^+	2964	3191
87 (305)	23 00 44.4	08 36 16	13.0	2.40	46	4790	4916
88 (305)	23 01 35.7	22 21 16	14.8	0.56^+	34^+	11,653	11,827
89 (91)	23 02 07.1	−08 57 20	14.5	0.40^+	42^+	14,380	...
90 (305)	23 25 24.4	08 30 13	13.6	1.75^+	25^+	8662	8747
91* (305)	23 33 40.5	01 52 46	13.1	2.70	42	2802	2795

KEY

Akn 42 7	Mrk 304 82	Mrk 612 24	Mrk 945 3	NGC 931 15
Akn 79 14	Mrk 308 84	Mrk 618 26	Mrk 955 4	NGC 1019 17
Akn 120 28	Mrk 315 88	Mrk 622 36	Mrk 993 8	NGC 2110 29
Akn 223 45	Mrk 335 1	Mrk 686 66	Mrk 1018 12	NGC 2992 43
Akn 232 47	Mrk 348 6	Mrk 700 75	Mrk 1044 16	NGC 3227 49
Akn 347 58	Mrk 374 33	Mrk 704 39	Mrk 1058 20	NGC 3516 53
Akn 564 85	Mrk 391 38	Mrk 705 41	Mrk 1066 21	NGC 4235 59
A0241+62 18	Mrk 403 42	Mrk 728 50	Mrk 1073 22	NGC 5548 64
A1058+45 51	Mrk 423 54	Mrk 739 55	Mrk 1098 68	NGC 5940 69
Mrk 3 31	Mrk 471 65	Mrk 744 56	Mrk 1126 86	NGC 6764 77
Mrk 6 32	Mrk 493 70	Mrk 766 60	Mrk 1146 5	NGC 6814 78
Mrk 9 34	Mrk 504 74	Mrk 789 62	Mrk 1157 9	NGC 7469 87
Mrk 50 61	Mrk 506 76	Mrk 841 67	Mrk 1218 37	NGC 7674 90
Mrk 78 35	Mrk 509 79	Mrk 871 72	Mrk 1239 44	NGC 7714 91
Mrk 110 40	Mrk 573 11	Mrk 883 73	Mrk 1243 46	T1059+105 52
Mrk 141 48	Mrk 590 13	Mrk 896 80	Mrk 1310 57	UGC 3255 27
Mrk 268 63	Mrk 595 19	Mrk 915 83	MCG 2-58-22 89	V Zw 85 10
Mrk 298 71	Mrk 609 23	Mrk 938 2	MCG 8-11-11 30	II Zw 136 81
				0335+09 25

1 ..... Mrk 335	19 ..... Mrk 595	37 ..... Mrk 1218	55 ..... Mrk 739	73 ..... Mrk 883
2 ..... Mrk 938	20 ..... Mrk 1058	38 ..... Mrk 391	56 ..... Mrk 744	74 ..... Mrk 504
3 ..... Mrk 945	21 ..... Mrk 1066	39 ..... Mrk 704	57 ..... Mrk 1310	75 ..... Mrk 700
4 ..... Mrk 955	22 ..... Mrk 1073	40 ..... Mrk 110	58 ..... Akn 347	76 ..... Mrk 506
5 ..... Mrk 1146	23 ..... Mrk 609	41 ..... Mrk 705	59 ..... NGC 4235	77 ..... NGC 6764
6 ..... Mrk 348	24 ..... Mrk 612	42 ..... Mrk 403	60 ..... Mrk 766	78 ..... NGC 6814
7 ..... Akn 42	25 ..... 0335+09	43 ..... NGC 2992	61 ..... Mrk 50	79 ..... Mrk 509
8 ..... Mrk 993	26 ..... Mrk 618	44 ..... Mrk 1239	62 ..... Mrk 789	80 ..... Mrk 896
9 ..... Mrk 1157	27 ..... UGC 3255	45 ..... Akn 223	63 ..... Mrk 268	81 ..... II Zw 136
10 ..... V Zw 85	28 ..... Akn 120	46 ..... Mrk 1243	64 ..... NGC 5548	82 ..... Mrk 304
11 ..... Mrk 573	29 ..... NGC 2110	47 ..... Akn 232	65 ..... Mrk 471	83 ..... Mrk 915
12 ..... Mrk 1018	30 ..... MCG 8-11-11	48 ..... Mrk 141	66 ..... Mrk 686	84 ..... Mrk 308
13 ..... Mrk 590	31 ..... Mrk 3	49 ..... NGC 3227	67 ..... Mrk 841	85 ..... Akn 564
14 ..... Akn 79	32 ..... Mrk 6	50 ..... Mrk 728	68 ..... Mrk 1098	86 ..... Mrk 1126
15 ..... NGC 931	33 ..... Mrk 374	51 ..... A1058+45	69 ..... NGC 5940	87 ..... NGC 7469
16 ..... Mrk 1044	34 ..... Mrk 9	52 ..... T1059+105	70 ..... Mrk 493	88 ..... Mrk 315
17 ..... NGC 1019	35 ..... Mrk 78	53 ..... NGC 3516	71 ..... Mrk 298	89 ..... MCG 2-58-22
18 ..... A0241+62	36 ..... Mrk 622	54 ..... Mrk 423	72 ..... Mrk 871	90 ..... NGC 7674
				91 ..... NGC 7714

TABLE 1—*Continued*

F_H ($10^6 M_\odot$ Mpc^{-2}) (8)	ΔV_{20} (km s^{-1}) (9)	$\Delta V_{20}(0)$ (km s^{-1}) (10)	M_H ($10^9 M_\odot$) (11)	L_B ($10^{10} L_\odot$) (12)	M_i ($10^{10} M_\odot$) (13)	M_H/L_B (14)	M_H/M_i (in solar units) (15)	M_i/L_B (16)
0.45 ± 0.12	299	396	16.6	12.6	21.7	0.13	0.08	1.7
0.38 ± 0.19	376	551	2.7	3.4	29.0	0.08	0.01	8.5
<0.05	...	...	<2.0	18.7	...	<0.01	...	...
<0.09	...	...	<3.3	7.8	...	<0.04	...	...
0.35 ± 0.09	215	...	13.1	13.7	...	0.10	...	...
0.40 ± 0.07	60	...	14.4	7.5	...	0.19	...	...
0.80 ± 0.17	681	...	31.7	7.3	...	0.43	...	...
0.38 ± 0.14	497	523	13.2	15.3	14.0	0.09	0.09	0.9
<0.07	...	...	<3.1	7.2	...	<0.04	...	...
<0.14	...	...	<5.8	2.5	...	<0.23	...	...
<0.19	...	...	<7.2	6.9	...	<0.10	...	...
<0.12	...	...	<6.2	13.0	...	<0.05	...	...
3.85 ± 0.54	289	367	9.4	4.0	10.2	0.24	0.09	2.5
6.87 ± 0.52	134	...	5.9	2.9	...	0.20	...	...
<0.54	...	...	<19.1	42.6	...	<0.04	...	...
<0.50	...	...	<11.1	2.9	...	<0.38	...	...
<0.40	...	...	<45.5	71.7	...	<0.06	...	...
<0.35	...	...	<46.2	43.6	...	<0.11	...	...
1.30 ± 0.54	376	459	23.4	4.9	11.6	0.48	0.20	2.4
0.76 ± 0.12	492	684	12.7	6.0	19.1	0.21	0.07	3.2
0.97 ± 0.19	315	400	19.7	9.2	14.5	0.21	0.14	1.6
1.86 ± 0.31	214	314	6.7	1.1	2.4	0.61	0.28	2.2
0.50 ± 0.05	395	549	5.7	9.6	32.9	0.06	0.02	3.4
0.38 ± 0.07	297	531	17.0	14.0	17.1	0.12	0.10	1.2
<0.52	...	...	<36.2	24.5	...	<0.15	...	...
1.37 ± 0.12	344	...	40.8	17.1	...	0.24	...	...
2.90 ± 0.17	264	395	10.5	3.4	11.4	0.31	0.09	3.4

NOTES ON INDIVIDUAL GALAXIES

Mrk 335 = A0003+19.

Mrk 938.—Close interacting pair. Bright companion ~5.4 to NNE, fainter companion ~5.6 to SSW (MW).

Mrk 945.—Spherical with pronounced corona (M). No companions (MW).

Mrk 955.—SB (M). Only much fainter galaxies nearby (MW).

Mrk 1146 = UGC 00488.—Sa–b (N). Companion at 3.6, P.A. 68°, size 0.7: × 0.4 (N).

Mrk 348 = UGC 00499 = NGC 262.—SA(s)0: (V), S0 (N), SA(s)a (SSS). Companion at 1.1, P.A. 326°, size 0.3 × 0.1; companion at 1.2, P.A. 86°, 0.5 × 0.25 (N).

Akn 42 = UGC 00959.—Sa: (N). Disturbed? Probably interacting with companion at 0.85, P.A. 256°, size 0.15 × 0.15. 0122.0+3159 at 4.2, P.A. 14°, size 0.7 × 0.4 (N).

Mrk 993 = UGC 00987.—Sa (N). No companions (MW).

Mrk 1157 = NGC 591 = UGC 01111.—SB0/SBa (N). Bright bar, size 0.7 × 0.35 (N). No companions (MW).

V Zw 85.—Compact. Group of three. (1) = Blue posteruptive Sb, patchy spherical disk, extended halo E. (2) = 25″ to NNE of (1), very red elliptical compact, m_p = 18.1. (3) 60″ to E of (1), blue elliptical compact, m_p = 17.7 (Z).

Mrk 573 = UGC 01214 = A0141+02.—S0 (N), SAB0 (V). Companion 4.9, P.A. 15°, size 0.5 × 0.3 (N).

Mrk 1018 = UGC 01597.—S0 (N). Of oval shape with faint corona (M).

Mrk 590 = NGC 863 = UGC 01727.—Sa (N). Pair with UGC 01713 (N), which lies 14′ away in P.A. 282°. Small elliptical galaxy 1′ to W (A).

Akn 79 = UGC 01757.—S: (N).

NGC 931 = UGC 01935 = Mrk 1040.—Sb (N). Companion superposed at 0.35, P.A. 353°, size 0.2 × 0.1 (N).

Mrk 1044.—Spheroidal with sharp boundaries, surrounded by a faint but extended envelope (M). No companions (MW).

NGC 1019 = UGC 02132.—SBb (N). In a dense part of a cluster (N). 0235.8+0145 at 3.7, P.A. 351°, size 0.6 × 0.45, m = 15.6 (N).

A0241+62.—QSO.

Mrk 595.—Spheroidal with faint corona (M).

Mrk 1058.—Central part of SB? No companions (MW).

Mrk 1066 = UGC 02456.—SB0 (N). Apparently a close double system (M).

Mrk 1073 = UGC 02608.—SBb (N). Disturbed? Bar 0.45 × 0.20, pair with UGC 02612 at 4.1, P.A. 145°. Companion at 3.3, P.A. 221°, size 0.5 × 0.3 (N).

Mrk 609.—S(A). Mrk 610 lies 1.8 to NE. Bright galaxy 4.1 to SW, fainter galaxy 4.0 to SSW (MW).

Mrk 612 = A0238−03.—Sperical with almost rectilinear ejections to E and W (M).

0335+09.—Compact bright center plus extended halo. Companion ~3.2 to ESE plus a number of fainter ones (MW).

Mrk 618 = A0434−10.—SB (A). Smaller irregular companion 47″ to N (A).

UGC 03255.—SB?b: (N).

Akn 120 = Mrk 1095 = UGC 03271.—Spheroidal. Seems to have a faint envelope, and an amorphous arc can be seen in NW (M).

NGC 2110.—E (MW).

MCG 8-11-11 = UGC 03374.—SB (N). Bright stellar nucleus in a diffuse bar (N).

Mrk 3 = UGC 03426 = A0609+71B.—S0 (N), SB0 (SSS). Pair with UGC 03422, which is 6.5 to NW (N). Fainter galaxy 9.6 to NE.

Mrk 6 = IC 450 = UGC 03547.—S0–a (N). Pair with UGC 3550 = IC 451 at 4.2 (N).

Mrk 374.—S(A).—Distorted barred spiral 68″ to SE (A). Interacting system (M).

Mrk 9 = A0732+58.—S? (A), S0P? (V).

Mrk 78 = A0737+65.—E? (MW). Companion 3.0 to SE (MW).

Mrk 622 = UGC 04229 = A0804+39.—Spheroidal with corona (M). Companion 2.9 to W (MW).

Mrk 1218 = NGC 2622.—S (M). Two fainter companions at 1.1 and 1.3 to SW (MW).

Mrk 391 = NGC 2691 = UGC 04664.—Sa? (N), SB(r)0 (SSS). Companion at 3.1, P.A. 75°, size 0.35 × 0.35 (N).

Mrk 704.—Spheroidal (M). No companions (MW).

Mrk 110.—Disturbed system with long straight jet to NW and shorter curved counter-jet (A).

Mrk 705 = Akn 202 = UGC 05025 = VIII Zw 47.—S0? (N). Singular, very bright nuclear region in ring (N).

NOTES ON INDIVIDUAL GALAXIES—*Continued*

Mrk 403 = A0937+21.—Spheroidal, compact (M). Companions 4.7 to E, 4.4 to ESE, 3.5 to NW, and 3.1 to E (MW).

NGC 2992.—SaP (V). Interacting pair with NGC 2993 at 2.9. Faint outer extensions with knots at ends (V).

Mrk 1239.—Spherical, compact (M). Companion 1.3 to SSW (MW).

Akn 223.—Compact, dust lane? Faintish spiral companion 2.9 to NE (MW).

Mrk 1243 = NGC 3080 = UGC 05372.—Sa (N). Pair with UGC 05371 at 4.4, P.A. 319° (N).

Akn 232.—Extremely compact. Fainter companion 1.3 to E (MW).

Mrk 141 = A1015+64.—SB? (A), E3? (V). Companion, an irregular barred spiral, lies 30″ to NW. Another companion, a late-type barred spiral, lies 105″ to NE. In cluster? (A).

NGC 3227 = UGC 05620.—Sb (N), SAB(s)aP (V). Interacting pair with NGC 3226 (V).

Mrk 728.—Compact, spheroidal (M). Companion 3.1 to SW, faint galaxies to E (MW).

A1058+45 = UGC 06100.—Sa? (N). No companions (MW).

T1059+105.—Starlike nucleus with fuzz. In group or cluster. Several companions (MW).

NGC 3516 = UGC 06153.—SB0 (N), (R′)SB(s)0/a (SSS). 1102.5+7246 at 4.6, P.A. 236°, size 0.35 × 0.30, m = 15.4 (N).

Mrk 423 = A1124+35.—Fainter companion at 3.3 to NE. Cluster at more than 5′ to NW (MW).

Mrk 739 = NGC 3758.—Close binary system (M). Companions 5.5 to NW and 5.3 to S.

Mrk 744 = NGC 3786 = UGC 06621.—SAB(rs)aP (V). Interacting pair with NGC 3788 at 1.5, P.A. 20°. 1136.8+3209 at 4.7 to SW, size 0.8 × 0.4 (N).

Mrk 1310.—Oval, compact (M). Faint companions 5.6 to NE and 4.0 to W (MW).

Akn 347 = NGC 4074.—Bright companion 4.6 to NW. Several bright galaxies 5′–10′ distant (MW).

NGC 4235 = IC 3098 = UGC 07310.—SA(s)asp (V). Noninteracting pair with NGC 4246 at 12′, NGC 4247 at 13′ (V).

Mrk 766 = NGC 4253 = UGC 07344.—(R′)SB(s)a? (V), (R′)SB0/a (SSS). Pair with NGC 4245 at 16.5 (V).

Mrk 50 = A1220+02.—Fairly compact (MW). Amorphous (A). No obvious companions (MW).

Mrk 789 = VIII Zw 323.—Spheroidal, fairly condensed (M). Faint companions ~6′ to N and S (MW).

Mrk 268.—Spheroidal with elongated envelope (M). Annular appearance (A). Companion at 53″ to NE. Companion 54″ to SE (A).

NGC 5548 = UGC 09149.—(R′)SA(s)0/a (V), Sa (N). No companions (MW).

Mrk 471 = UGC 09214 = A1420+33.—SBa (N). Spheroidal formation (M). Two pronounced spiral arms (A). No companions (MW).

Mrk 686 = NGC 5695 = UGC 09421.—S (N). No companions (MW).

Mrk 841.—Very condensed (M). Faintish companion 4.7 to E (MW).

Mrk 1098.—Spherical, compact (M). Companions 1.5 to SW, 3.4 to E (MW).

NGC 5940 = UGC 09876.—SBa–b (N). Fainter companion 4.8 to E (MW).

Mrk 493 = UGC 10120 = A1557+35.—SBb (N). No companions (MW).

Mrk 298 = UGC 10192 = IC 1182.—S0$^+$P (V). Disturbed object, with long knotty plume extending 1.3 to E. In Hercules Cluster (A, V, N).

Mrk 871 = IC 1198.—S(M). No companions (MW).

Mrk 883.—Spheroidal, moderately condensed (M). Curious ring-shaped feature to SW. No companions (MW).

Mrk 504 = A1659+29.—SB? E6? (M). Similar barred spiral with ring lies 1.8 to NW (A).

Mrk 700 = UGC 10675.—Double system, plume, very long bridge (N).

Mrk 506 = A1720+30.—SAB(r)a (V). Elliptical companion (E5) of comparable size and redshift 40″ to SW, but no obvious signs of interaction (A).

NGC 6764 = UGC 11407.—SB(s)b (V), SB(s)bc (N). Companion at 2.6, P.A. 110°, size 0.4 × 0.3, E–S0. Companion at 4.5, P.A. 32°, size 0.8: × 0.2 (N).

NGC 6814.—SAB(rs)bc (V), SAB(rs)b (SSS). No companion (MW).

Mrk 509.—Bright nucleus surrounded by faint, apparently structureless envelope (A).

Mrk 896.—Close pair with undivided components (M). No companions (MW).

II Zw 136 = UGC 11763.—Very blue spherical, very compact (Z).

Mrk 304 = II Zw 175.—Very blue spherical, very compact (Z).

Mrk 915.—Spheroidal with faint corona (M). Bright companion 4.3 to SW. Companion 2.1 to SE. Faint galaxies 5.5 to NE and 5.3 to SSW (MW).

Mrk 308 = A2239+19.—I0? (V). Companion 0.9 to NE. Companion 4.0 to E (MW).

Akn 564 = UGC 12163 = A2240+29.—SB (N). No companions (MW).

Mrk 1126 = NGC 7450.—S? (MW). No companions (MW).

NGC 7469 = UGC 12332.—(R′)SAB(rs)a (V), (R′)SB(rs)a (SSS). Pair with IC 5283 at 1.4, P.A. 25°, size 0.7 × 0.25.

Mrk 315 = II Zw 187 = A2301+22.—E1P? (V). Blue, large, patchy, fuzzy, compact (Z). Companion 3.6 to E (MW).

MCG 2-58-22 = Mrk 926.—Spherical, with appreciable halo. 1′ to S is a fairly compact satellite(?) galaxy (M).

NGC 7674 = Mrk 533 = UGC 12608.—SA(r)bcP (V), SBb (N). Pair with galaxy at 0.6, P.A. 64°, size 0.2 × 0.15. NGC 7675 at 2.5, P.A. 105°, size 0.5 × 0.3, E. Companion at 3.7, P.A. 250° size 0.4 × 0.2 (N).

NGC 7714 = Mrk 538 = UGC 12699.—SB(s)b:P (V). Interacting pair with NGC 7715 at 1.9 (V).

REFERENCE CODE

A = Adams 1977. M = original Markarian discovery papers. MW = inspection of PSS by present authors. N = Nilson 1973. SSS = Simkin, Su, and Schwarz 1980. V = de Vaucouleurs, de Vaucouleurs, and Corwin 1976. Z = Zwicky 1971.

detected in H I, it was not possible to derive an inclination in eight cases.

Col. (6).—Optical velocity, $V_{\rm opt}$, in km s^{-1}, as given by Khachikian and Weedman (1974), Weedman (1977), and Huchra (1982). For redshifts derived from Western sources, the values quoted represent $c\Delta\lambda/\lambda$ (heliocentric). It is probable that the same is true for the (few) values originally taken from Soviet publications, but this is often not explicitly stated.

Col. (7).—Neutral hydrogen heliocentric velocity, $V_{\rm H\,I}$ (i.e., $c\Delta\lambda/\lambda$), in km s^{-1}, taken as the flux-weighted mean velocity over the profile between the first and last channels of the hydrogen signal. This definition is preferred because a large fraction of the Seyfert galaxies are likely to have perturbations of their internal dynamics as well as high-velocity H I streams due to tidal interactions with close companions. For the 25 Arecibo detections, we computed the heliocentric velocity $V_{\rm H\,I}$ using several definitions and find no substantial statistical differences. The mean difference between the flux-weighted velocities and the midpoint velocities at the 20% fractional level of the peak intensity signal is -0.7 ± 3.2 km s^{-1}. The mean difference between the flux-weighted velocities and the midpoint velocities at the 20% fractional level of the mean intensity of the signal is $+3.1 \pm 5.3$ km s^{-1}. The galaxies NGC 7469 and NGC 7674 show prominent absorption. For NGC 7469 the differences between the heliocentric velocities computed in these three different ways are as small as the velocity resolution of our observations. For NGC 7674 only the flux-weighted mean velocity over the emission signal is given.

Col. (8).—Observed integrated hydrogen flux density, $F_{\rm H}$, and its error, in units of $10^6\ M_\odot$ Mpc^{-2}. This quantity was calculated from

$$F_{\rm H} = 0.236 \int S dv\ (10^6\ M_\odot\ {\rm Mpc}^{-2})\,, \qquad (5)$$

where S is the flux density in Jy, and dv is in km s^{-1} (e.g., Fisher and Tully 1981). The uncertainties in F_H were estimated by multiplying the channel-to-channel rms by the observed width of the signal. For strong signals, the uncertainties are determined by errors in the calibration. At Arecibo, galaxies with well-known H I profiles were regularly observed in order to test the calibration procedures. For the test galaxy NGC 7080 we obtained four profiles with signal-to-noise ratios of ~ 10 during different observing periods. The comparison of the integrated fluxes for these profiles gives a maximum dispersion of 10%. The comparison of our Arecibo integrated fluxes with NRAO 91 m telescope integrated fluxes measured by Rubin *et al.* (1976) for the galaxies NGC 7080, IC 509, and the galaxy 153 of their list gives differences of 12%, 23%, and 10%. We estimate that the calibration uncertainties for the 305 m observations may introduce a maximum error of $\sim \pm 25\%$ in the H I fluxes.

Using the 91 m telescope, we obtained profiles with signal-to-noise ratios greater than 10 for the program galaxies Mrk 348 and NGC 7674. A comparison with the integral fluxes for these two galaxies obtained by HBS shows differences of 11% and 13%. We estimate that the maximum uncertainty in the H I fluxes of the 91 m profiles due to calibration errors is $\pm 20\%$. We point out that in some profiles with low signal-to-noise ratio, errors due to baseline-fitting uncertainties may dominate and be larger than the errors listed in Table 1. Upper limits were calculated by multiplying the channel-to-channel rms by an assumed width of 300 km s^{-1}.

Col. (9).—Velocity width, ΔV_{20}, at the 20% level of the average emission between the first and last channels of the hydrogen signal, in km s^{-1}. For the Arecibo observations, a comparison with the velocity widths at the 20% level of the peak intensity of the signal over the same window shows that the latter are on the average 13% smaller. We made no corrections by the relativistic $(1+z)^{-1}$ factor, which is smaller than 4.0% for the sample of detected galaxies.

Col. (10).—Velocity width, ΔV_{20}, at the 20% level of the average emission, corrected for inclination and in km s^{-1}. The inclination correction followed

$$\Delta V_{20}(0) = \Delta V_{20}/\sin i \, . \tag{6}$$

For galaxies close to face-on ($i < 31°$), no inclination correction was applied.

Col. (11).—Mass of neutral hydrogen, M_H, in units of $10^9\, M_\odot$. We first derived the integrated hydrogen flux density, F_c, corrected for resolution effects according to the formula (Sullivan *et al.* 1981)

$$F_c = F_H\{1 + [0.7a_H(0)/\theta]^2\}^{1/2}\{1 + [0.7b_H(0)/\theta]^2\}^{1/2} \, , \tag{7}$$

where $\theta = 3'.3$ for the Arecibo observations, and $\theta = 10'.8$ for the NRAO observations. We emphasize that corrections, such as this one, are quite uncertain, even for galaxies as small as 2′–3′. The hydrogen mass follows from

$$M_H = F_c D^2 \, M_\odot \, , \tag{8}$$

where D is the distance in Mpc, derived from the recession velocity with respect to the velocity centroid of the Local Group of galaxies (RCBG2) and a Hubble constant $H_0 = 55$ km s^{-1} Mpc^{-1}.

Col. (12).—Blue luminosity, L_B, in units of $10^{10}\, L_\odot$. The magnitudes (col. [3]) were first converted into total blue magnitudes using equation (7) of Fisher and Tully (1981). Corrections for internal and Galactic obscuration (eqs. [10]–[12] of Fisher and Tully 1981) were then applied, and the blue luminosity, in solar units, was calculated assuming M_B (Sun) = 5.48. The value of L_B given includes contributions from both the nucleus and the galaxy disk.

The blue luminosity for galaxies with $m > 14.5$ may be overestimated by 0.5 mag when using converted Zwicky magnitudes (Bothun and Schommer 1982). Since $\sim 50\%$ of the galaxies in our sample have $m > 14.5$, the quantity M_H/L_B may be biased toward lower values in many galaxies.

Col. (13).—Total indicative mass, M_i, in units of $10^{10}\, M_\odot$. This represents an estimate of the total mass of the galaxy determined from the H I line width:

$$M_i = 5000 D a_H(0) \Delta V_{20}(0)^2 \, . \tag{9}$$

Here D is the distance in Mpc, the units of $a_H(0)$ are arcmin, and those of $\Delta V_{20}(0)$ are km s^{-1} (Sullivan *et al.* 1981).

Col. (14).—Hydrogen mass to blue luminosity ratio, M_H/L_B. Because our values of L_B include nuclear light, the numbers given may be systematically lower than M_H/L_B for the galaxy disk alone.

Col. (15).—Hydrogen to total mass ratio, M_H/M_i.

Col. (16).—Total mass to blue luminosity ratio, M_i/L_B.

The notes section below Table 1 gives alternate designations for galaxies listed in more than one of the better known catalogs. Immediately following the name is the morphological type, when available, and information on peculiarities and the presence of companion galaxies. Sometimes different authors list different morphological types; in these cases, each type estimate is given. For the galaxies examined by the authors on the PSS prints to determine sizes and axial ratios, remarks on morphology and the presence of companion galaxies are given. Additionally, all galaxies detected in H I were searched for companions; this search was restricted to a radius of 5 mm (= 5′.6) from the galaxy, and galaxies much fainter than the program galaxy were, in general, not listed. We emphasize the great difficulty in classification of many of our program galaxies in any morphological system (cf. discussion in Adams 1977), because of contamination by the bright nucleus and the unfavorable spatial scale of the more distant systems (1″ $\approx$ 1 kpc at recession velocity = 11,000 km s^{-1} with $H_0 = 55$ km s^{-1} Mpc^{-1}). References for the information are given in parentheses, according to the code at the end of the notes.

There are 21 galaxies in common with our survey and that performed by HBS. For 17 of these galaxies, of which seven were detected in H I, the results of the two surveys are in excellent agreement. The four discrepant galaxies are Mrk 590, Mrk 3, NGC 5548, and Mrk 298. The hydrogen masses of Mrk 3 and NGC 5548 differ by factors of between 2 and 3. The absorption suspected by HBS in NGC 5548 is not apparent in our profile. Our upper limit for Mrk 590 is slightly below the mass given by HBS. The only serious discrepancy concerns Mrk 298, for which our mass is a factor of 4.6 larger than their upper limit. Schommer, Sullivan, and Bothun (1981) and Bothun, Stauffer, and

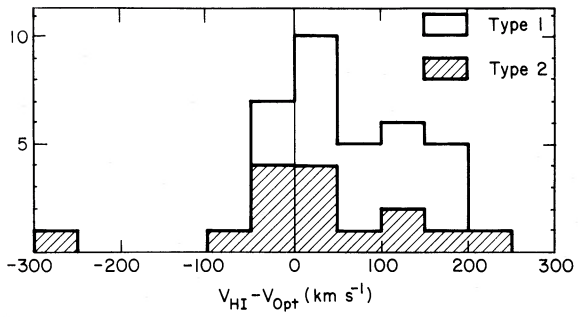

FIG. 2a

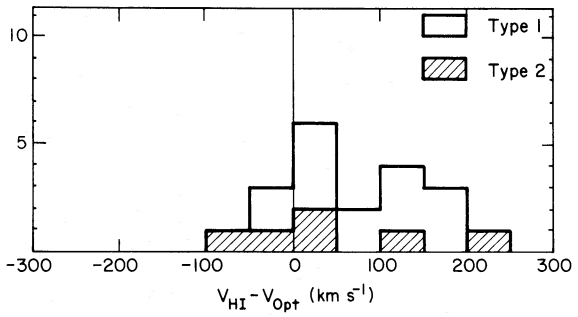

FIG. 2b

FIG. 2.—(*a*) Histograms of the difference between the H I and optical nuclear redshifts for 36 Seyfert galaxies. The objects plotted comprise all the detected galaxies in Table 1, except Mrk 3, Akn 223, and NGC 7714 (see § IV*a*). (*b*) As Fig. 2*a*, but for 20 galaxies with no companions within the telescope beam.

Schommer (1981) give an H I mass for this galaxy similar to our value (after allowing for the H_0 assumed). Our results are also in good agreement with those of Bieging and Bierman (1983) for the 10 galaxies in common with the two surveys. The hydrogen flux determined for NGC 6764 by Fisher and Tully (1981) is within 5% of our measurement.

IV. H I PROPERTIES OF THE OBSERVED GALAXIES

a) Radial Velocities

A comparison of our H I redshifts with the optical nuclear redshifts can provide some insight on the motion of gas in the nuclear regions of Seyfert galaxies. It is known that the bulk of the neutral hydrogen in galaxies is spread throughout the galaxy, so the H I profiles should provide a good indication of the systemic velocity. On the other hand, the optical emission lines reflect the movement of gas in the nuclear regions. In the following we compare the optical and radio redshifts of Seyfert galaxies. We exclude Mrk 3, Akn 223, and NGC 7714 from this analysis since interferometric observations show that the H I measured in the direction of Mrk 3 is actually in a gas-rich companion galaxy (A. G. de Bruyn, private communication to Heckman *et al.* 1981), and Akn 223 and NGC 7714 are not Seyfert galaxies.

Figure 2*a* is a histogram of the velocity difference between the H I and optical emission lines for 36 H I–detected galaxies from Table 1. The distribution of $V_{HI} - V_{opt}$ is asymmetric, with a trend for the radio redshifts to be greater than the optical. There are 27 galaxies with $V_{HI} > V_{opt}$, and only nine galaxies with $V_{HI} < V_{opt}$. The mean value of $V_{HI} - V_{opt}$ is $+58$ km s^{-1}, and the standard deviation of the mean is ± 15 km s^{-1}. For the type 1's (21 galaxies) the mean and its standard deviation are $+76$ and ± 15 km s^{-1}, respectively; for the type 2's (15 galaxies) these numbers are $+32$ and ± 30 km s^{-1}. The highly discrepant galaxy in Figure 2*a* is Mrk 1239, which has a $V_{HI} - V_{opt}$ of -274 km s^{-1}. Synthesis observations of this object are desirable to check whether the neutral hydrogen is in the Seyfert or the companion galaxy $\sim 1'.3$ away.

Among the H I–detected galaxies, there are several instances of galaxies with close companions within the telescope beam (see notes to Table 1). If these cases are omitted, the histogram in Figure 2*b* is obtained, and here the tendency for positive values of $V_{HI} - V_{opt}$ is also strong. There are 16 galaxies with $V_{HI} > V_{opt}$ and four galaxies with $V_{HI} < V_{opt}$. Considering all 20 galaxies, the mean and standard deviation of $V_{HI} - V_{opt}$ are $+74$ and ± 18 km s^{-1}. For the type 1's (14 galaxies), we find $+80 \pm 21$ km s^{-1}, and for the type 2's (six galaxies), $+61 \pm 43$ km s^{-1}.

HBS reported no statistically significant difference between the H I and optical redshifts. However, their list included a few objects whose Seyfert classification has since been rescinded, as well as a number of Seyfert galaxies with close companions. Excluding these objects, only ~ 10 Seyfert galaxies with H I detections remain, which is too small a sample to exhibit any statistically significant trend. The mean velocity difference, $V_{HI} - V_{opt}$, for these galaxies is $+23$ km s^{-1} with a dispersion in the mean of 60 km s^{-1}.

There are three possible explanations, which we now discuss in turn, for this trend of V_{HI} to be greater than V_{opt}: (i) There are systematic errors in the H I redshifts. (ii) There are systematic errors in the optical redshifts. (iii) The effect is real and represents a difference between the mean radial velocity of the optical ionized material and the neutral hydrogen, the latter presumably representing the systemic velocity.

With regard to the possibility of systematic errors in the H I redshifts, analysis shows the same significant trend in both Arecibo and NRAO data, so the effect does not depend on the data-taking and reduction procedures. Furthermore, we obtain the same systematic difference between the H I and optical redshifts whether we use the average of the two velocities at which the H I profile falls to 20% or the flux-weighted mean H I velocity (§ III). Also, regular observations of eight test non-Seyfert galaxies with well-known H I profiles show an excellent agreement with published data. We conclude that the tendency toward positive values of $V_{HI} - V_{opt}$ is not a consequence of systematic errors in the H I velocities.

To investigate the possibility of systematic errors in the optical velocities, comparison of H I and optical velocities has been made for different sources of optical data. Eighteen of our detected galaxies have velocities determined in the Harvard redshift survey (Huchra 1982); the mean of $V_{HI} - V_{opt}$ is $+31$, and its standard deviation is ± 25 km s^{-1}. Thirteen galaxies have optical velocities listed in the RCBG2; for these galaxies the mean of $V_{HI} - V_{opt}$ is $+55$ with standard deviation ± 54 km s^{-1}. Finally, 10 galaxies have redshifts

from various Soviet publications; here the mean of $V_{H\,I} - V_{opt}$ is +106 with standard deviation ±40 km s^{-1}. These large dispersions between H I and optical velocities are probably a consequence of the difficulty of optical redshift determination from broad and asymmetric emission lines. On the other hand, it is unclear how systematic errors could be common to all the above-mentioned optical measurements. Although this explanation cannot be ruled out, we do not find it attractive at the present time.

We tentatively favor a real difference between H I and optical redshifts. Optical observers have argued for many years that gas is moving radially, probably outward, in the central regions of Seyfert galaxies. If such outwardly moving line-emitting gas is mixed with dust, the attenuation of emission from the far side leads to an observed redshift below systemic. Alternatively, if the line-emitting clouds contain dust, are falling in toward the nucleus, and are ionized preferentially on the side closest to the central ionizing source, the same velocity difference will result. Heckman *et al.* (1981) also found that [O III] λ5007 tends to be blueshifted with respect to systemic velocity in a sample of nine galaxies, and they use the outflow model to account for the effect and the line asymmetries. Furthermore, Wilson (1979) and Osterbrock (1981) find that lines from more highly ionized species are broader and more blueshifted in certain objects, suggesting that higher expansion velocities are found closer to the nucleus.

Other evidence for high dust content in the narrow-line regions of Seyfert galaxies comes from measurements of optical polarization (e.g., Schmidt and Miller 1980) and the relative intensities of the narrow emission lines (e.g., Koski 1978). Unfortunately, there are too few measurements of the Balmer decrement to check for a correlation with $V_{H\,I} - V_{opt}$. Rieke (1978) suggests that the infrared continuum in Seyferts is predominantly thermal reradiation by dust. We have compared $V_{H\,I} - V_{opt}$ with the infrared luminosity measured by Rieke (1978) for 13 galaxies and find no evidence for correlation.

It is possible that the outflow of gas from the nucleus takes place along preferred directions with respect to the rotation axis of the galaxy. If this were the case, a correlation between $V_{H\,I} - V_{opt}$ and the inclination angle, i, of the galaxy might be expected. The data, however, show no correlation between these two quantities.

b) Hydrogen Masses and Hydrogen Mass to Light Ratios

The hydrogen masses, M_H, and blue luminosities, L_B, of galaxies in our survey cover a wide range; M_H extends from less than $5 \times 10^8\ M_\odot$ for NGC 4235 to $5.9 \times 10^{10}\ M_\odot$ for NGC 931, and L_B ranges between $7 \times 10^9\ L_\odot$ for Mrk 1310 and $7.2 \times 10^{11}\ L_\odot$ for II Zw 136.

The hydrogen mass to blue luminosity ratio, M_H/L_B, is a distance-independent parameter which varies from less than 0.01 in elliptical galaxies to values as large as 0.5 in late-type spiral galaxies. Figure 3 shows a plot of M_H/L_B versus morphological type for all the galaxies surveyed by us and HBS which have reasonably well determined types. The type classification, T, follows the system described in the RCBG2; i.e., S0 = −2, S0/a = 0, Sa = 1, Sa–b = 2, Sb = 3, and Sb–c = 4. Also shown in the diagram are the mean M_H/L_B ratios with their standard deviations (*vertical bars*) and the total range of M_H/L_B (*dashed lines*) in normal galaxies, as given by Balkowski (1973). Her hydrogen masses have been multiplied by the factor 1.3 to bring them to the same scale as Green Bank measurements. It should also be borne in mind that Balkowski's (1973) mean M_H/L_B for early-type systems is probably too high; for example, Gallagher, Faber, and Balick (1975) suggest a mean M_H/L_B for S0 galaxies

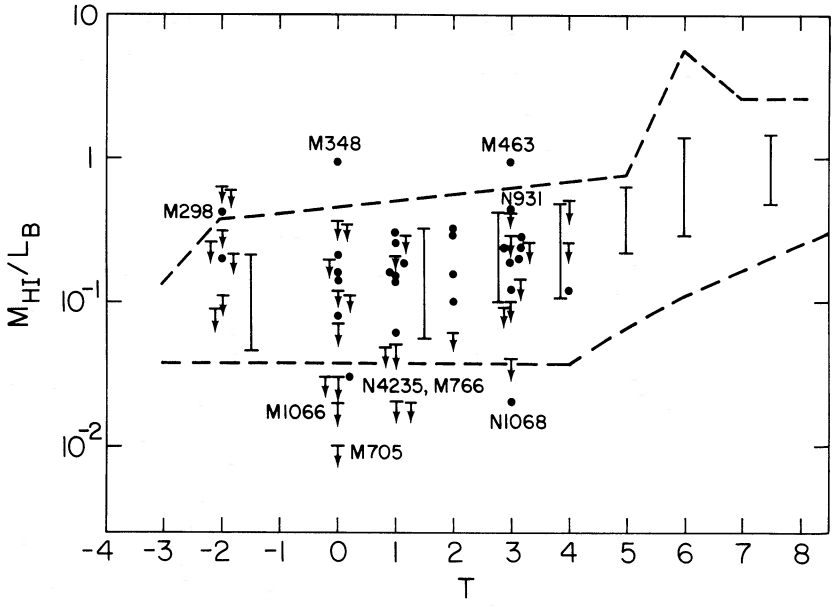

FIG. 3.—Plot of the hydrogen mass to blue luminosity ratio, M_H/L_B, against morphological type, according to the system in the RCBG2. The galaxies plotted are those Seyfert galaxies in Table 1 of this paper and Table 1 of HBS which have a type classification. Also shown are the mean M_H/L_B ratios with their standard deviations (*vertical bars*) and the total range of M_H/L_B (*dashed lines*) in normal galaxies, as given by Balkowski (1973).

of $\lesssim 0.06$, although these galaxies show a large range in M_H/L_B with the mean and standard deviation still being quite uncertain (Knapp *et al.* 1977). Also, the type classification for many of our galaxies may be in error, by ± 1 or ± 2 in T.

Despite these uncertainties, inspection of Figure 3 reveals the following. First, as is well known, Seyfert galaxies are restricted to early-type spirals, i.e., spirals with a prominent bulge component. Second, M_H/L_B for the great majority of Seyferts does not differ from the values expected for a normal galaxy of the same morphological type. As emphasized above, the low values for some Sa and S0/a galaxies, such as Mrk 1066 and Mrk 705, are probably not unusual. NGC 1068 has long been known to be deficient in H I; HBS discuss the possibility that much of the missing gas in this galaxy is actually in molecular form. On the other hand, there are several instances of galaxies with M_H/L_B ratios above 0.4. These objects are Mrk 938, Mrk 348, NGC 931, Mrk 298, Mrk 915, and Mrk 1126 (Table 1). Mrk 938 is a close interacting pair with an uncertain H I flux; errors in baseline fitting may contribute to the relatively large M_H/L_B ratio. The existence of a large and massive H I envelope around Mrk 348 was first noted by HBS and subsequently mapped by Morris and Wannier (1980) and by Heckman *et al.* (1982). The H I mass is $\sim 3 \times 10^{10}\ M_\odot$, and its extent ~ 240 kpc. NGC 931 is a type 1 Seyfert interacting with a small, gas-rich (as evidenced by strong optical emission lines) companion (Ward and Wilson 1979). The Holmberg diameter [$a_H(0) = 4'.45$] is larger than the Arecibo telescope beam, and, although a correction for resolution has been applied to the hydrogen masses, the M_H/L_B ratio of 0.45 may be an underestimate. Even so, with $M_H = 5.9 \times 10^{10}\ M_\odot$, NGC 931 has a higher hydrogen mass than any other galaxy in our survey. Its Holmberg diameter is ~ 120 kpc. The unusual H I properties of Mrk 298 have been discussed earlier by Bothun, Stauffer, and Schommer (1981).

Our data suggest that Seyfert galaxies show a larger total spread in M_H/L_B and M_H/M_i ratios for a given morphological type than do normal galaxies. Uncertainty in type and the absence of definitive comparison samples of early-type normal spiral galaxies preclude any quantitative discussion of this effect. We find no evidence for any systematic differences in the histograms of M_H/L_B or M_H/M_i ratios between type 1 and type 2 Seyfert galaxies.

c) H I *Absorption*

The radio continuum emission of Seyfert galaxies is associated with the nucleus of the galaxy and usually has a steep nonthermal spectrum, with about 10% exhibiting a flat-spectrum, very compact core (de Bruyn and Wilson 1978). For a number of Seyfert galaxies, H I absorption has been detected against their nuclear radio sources. These galaxies are NGC 1275 (de Young, Roberts, and Saslaw 1973), Mrk 6 (Haschick, Baan, and Burke 1976; HBS), NGC 4151, Mrk 231 (Dickey 1982), NGC 7469, NGC 7674 (Mirabel 1982; this paper), and NGC 5506 (Thuan and Wadiak 1982; Dickey 1982). The H I emission profile reflects the dynamics of the whole galaxy, while the H I absorption probes the motion of the clouds located on the near side of the radio source. The relative velocity shift between absorption- and emission-line velocities can provide a test for the idea that infalling H I of tidal origin may cause large-scale noncircular motions in the interstellar gas and also energize the central radio source. Of course, a displacement of absorption and systemic velocities can also arise through an asymmetric configuration of the compact radio source and the absorbing H I clouds or through stable noncircular orbits in barred spiral galaxies (e.g., Sanders and Tubbs 1980). Among Seyfert galaxies with good signal-to-noise spectra, four have the H I absorption signal redshifted by more than 40 km s^{-1} with respect to the systemic velocity, suggesting that infall is a common process. Only NGC 7674 shows the H I absorption signal blueshifted with respect to the emission centroid by more than 40 km s^{-1}.

d) *Line Shapes and Interacting Galaxies*

Inspection of Figure 1 shows that a significant number, perhaps 40% or more, of Seyfert galaxies exhibit H I profiles different from the typical symmetric, double-horned shape of an inclined normal spiral or the narrow line of a near face-on spiral. The notes to Table 1 indicate that most of the detected Seyfert galaxies have close companions or are part of interacting systems. Asymmetric profiles and extremely broad lines may be the result of (i) blended emission from more than one galaxy within the telescope beam, (ii) strong perturbations on the internal dynamics of the galaxies by the tidal interaction with close companions, or (iii) disturbance of the H I disk by the nuclear activity. Possible examples of phenomena (i) and (ii) may be found in the systems NGC 3227, Mrk 744, Mrk 298, NGC 7469, NGC 7674, and NGC 2992. A detailed analysis of these possibilities will require aperture-synthesis observations of the H I distributions.

We are grateful to Daniel Altschuler for his assistance with some of the 305 m observations. We also wish to thank the operations staffs of the NAIC and NRAO for their extensive help. Special thanks are accorded to Michael Davies and Murray Lewis of the NAIC and W. Brundage, B. Vance, and G. Martin of NRAO. J. P. Huchra provided his catalog of Seyfert galaxies in advance of publication, which proved invaluable in organizing our observing program. W. T. Sullivan III made useful comments on the original manuscript. The project was begun while I. F. M. was at the Astronomy Program, University of Maryland. I. F. M. is grateful to Professor Frank J. Kerr for his support through NSF grant AST 77-26898. A major part of this research was supported by NSF grant AST 80-13148 to the University of Puerto Rico.

REFERENCES

Adams, T. F. 1977, *Ap. J. Suppl.*, **33**, 19.
Apparao, K. M. V., Bignami, G. F., Maraschi, L., Helmken, H., Margon, B., Hjellming, R., Bradt, H. V., and Dower, R. G. 1978, *Nature*, **273**, 450.
Balkowski, C. 1973, *Astr. Ap.*, **29**, 43.
Bieging, J. H., and Biermann, P. 1983, *A.J.*, **88**, 161.
Bothun, G. D., and Schommer, R. A. 1982, *Ap. J.* (*Letters*), **255**, L23.
Bothun, G. D., Stauffer, J. R., and Schommer, R. A. 1981, *Ap. J.*, **247**, 42.
Clements, E. D. 1981, *M.N.R.A.S.*, **197**, 829.
Clements, E. D. 1982, private communication.
de Bruyn, A. G., and Wilson, A. S. 1978, *Astr. Ap.*, **64**, 433.
de Vaucouleurs, G., de Vaucouleurs, A., and Corwin, H. G., Jr. 1976, *Second Reference Catalogue of Bright Galaxies* (Austin: University of Texas Press).
de Young, D. S., Roberts, M. S., and Saslaw, W. C. 1973, *Ap. J.*, **185**, 809.
Dickey, J. M. 1982, *Ap. J.*, **263**, 87.
Dressel, L. L., and Condon, J. J. 1976, *Ap. J. Suppl.*, **31**, 187.

Fisher, J. R., and Tully, R. B. 1981, *Ap. J. Suppl.*, **47**, 139.
Gallagher, J. S., Faber, S. M., and Balick, B. 1975, *Ap. J.*, **202**, 7.
Gallouët, L., Heidmann, N., and Dampierre, F. 1975, *Astr. Ap. Suppl.*, **19**, 1.
Haschick, A. D., Baan, W. A., and Burke, B. F. 1976, *Bull. AAS*, **8**, 496.
Heckman, T. M., Balick, B., and Sullivan, W. T., III. 1978, *Ap. J.*, **224**, 745 (HBS).
Heckman, T. M., Miley, G. K., van Breugel, W. J. M., and Butcher, H. R. 1981, *Ap. J.*, **247**, 403.
Heckman, T. M., Sancisi, R., Sullivan, W. T., III, and Balick, B. 1982, *M.N.R.A.S.*, **199**, 425.
Huchra, J. 1982, Catalog of Seyfert Galaxies, preprint.
Joshi, M. N., and Kandalian, R. A. 1981, *Bull. Astr. Soc. India*, **9**, 24.
Keel, W. C. 1980, *A.J.*, **85**, 198.
Khachikian, E. Ye., and Weedman, D. W. 1974, *Ap. J.*, **192**, 581.
Knapp, G. R., Gallagher, J. S., Faber, S. M., and Balick, B. 1977, *A.J.*, **82**, 106.
Kojoian, G., Elliott, R., and Tovmassian, H. M. 1978, *A.J.*, **83**, 1545.
Koski, A. T. 1978, *Ap. J.*, **223**, 56.
Mirabel, I. F. 1982, *Ap. J.*, **260**, 75.
Morris, M., and Wannier, P. G. 1980, *Ap. J. (Letters)*, **238**, L7.
Nilson, P. 1973, *Uppsala General Catalogue of Galaxies* (Uppsala: Uppsala Astronomical Observatory).
Osterbrock, D. E. 1981, *Ap. J.*, **246**, 696.
Peterson, S. D. 1973, *A.J.*, **78**, 811.
Rieke, G. H. 1978, *Ap. J.*, **226**, 550.
Rubin, V. C., Ford, W. K., Thonnard, N., Roberts, M. S., and Graham, J. A. 1976, *A.J.*, **81**, 687.
Sanders, R. H., and Tubbs, A. D. 1980, *Ap. J.*, **235**, 803.
Schmidt, G. D., and Miller, J. M. 1980, *Ap. J.*, **240**, 759.
Schommer, R. A., Sullivan, W. T., III, and Bothun, G. D. 1981, *A.J.*, **86**, 943.
Simkin, S. M., Su, H. J., and Schwarz, M. P. 1980, *Ap. J.*, **237**, 404.
Su, H. J., and Simkin, S. M. 1980, *Ap. J. (Letters)*, **238**, L1.
Sullivan, W. T., III, Bothun, G. D., Bates, B., and Schommer, R. A. 1981, *A.J.*, **86**, 919.
Thuan, T. X., and Wadiak, E. J. 1982, *Ap. J.*, **252**, 125.
Tovmassian, H. M., Shahbazian, E. Ts., and Kandalian, R. A. 1980, *Soob. Byurakan Obs.*, **52**, 58.
Ward, M. J., and Wilson, A. S. 1979, *Astr. Ap.*, **70**, L79.
Weedman, D. W. 1977, *Ann. Rev. Astr. Ap.*, **15**, 69.
———. 1978, *M.N.R.A.S.*, **184**, 11p.
Wilson, A. S. 1979, *Proc. Roy. Soc. London, A*, **366**, 461.
Wilson, A. S., and Meurs, E. J. A. 1978, *Astr. Ap. Suppl.*, **33**, 407.
Zwicky, F. 1971, *Catalogue of Selected Compact Galaxies and of Post-eruptive Galaxies*, published by F. Zwicky.
Zwicky, F., *et al.* 1961–1968, *Catalogue of Galaxies and of Clusters of Galaxies*, Vols. **1–6** (Pasadena: California Institute of Technology).

I. F. MIRABEL: Department of Physics, University of Puerto Rico, Box AT, University Station, San Juan, PR 00931

A. S. WILSON: Astronomy Program, University of Maryland, College Park, MD 20742